Local Heat Flux Similarity between Hypersonic Flight and Plasma Wind Tunnel

P. F. Barbante⋆
⋆*Politecnico di Milano, Dept. of Mathematics*
P.zza Leonardo da Vinci 32, 20133 Milano, Italy
paolo.barbante@polimi.it

Abstract

Development of reusable space vehicles requires a precise qualification of their Thermal Protection System materials. The catalytic properties should be determined in plasma wind tunnels for test conditions relevant to the real flight mission program. However perfect reproduction of the flight environment is practically impossible for reacting flows and one is obliged to resort to a partial simulation. In an attempt to overcome such an issue we present the Local Heat Flux Similarity theory that allows to establish under which hypothesis and approximations the flow field inside a ground facility is equivalent to the real one experienced by a space vehicle.

1. Introduction

Design and testing of Thermal Protection System (TPS) materials for aerospace vehicles are a major issue for the definition of space missions. The determination of the catalytic properties of TPS materials is crucial for the design of an optimal flight strategy: by a matter of fact the heat flux for a fully catalytic wall can be more than twice the heat flux for a noncatalytic one. This situation requires ground facilities able to provide representative testing conditions for the evaluation of the material performances; because TPS materials should be tested in real flight conditions, in order to safely rely on their catalytic properties. However it is also well known that complete similarity is possible for reacting flows only if the flight environment, including vehicle dimensions, is fully reproduced in the wind tunnel. The usual strategy to overcome such a problem is to resort to some kind of partial simulation: only some characteristics of the flight environment, that are of interest in the specific experiment, are reproduced.

In this contribution we present a theory, called Local Heat Flux Similarity, that allows to establish under which hypothesis and approximations the flow field inside a plasma wind tunnel is able to reproduce the real one experienced by a re-entry vehicle. The focus, as implied by theory name, is on heat flux duplication between flight and ground facility. In Ref. 1 we presented a methodology for local heat flux similarity in the stagnation region; here we extend the previous work to the whole boundary layer.

2. Local heat flux similarity concept

The purpose of this section is to derive, for wall heat flux, an analytical expression that can be used to establish heat flux similitude between real flight and wind tunnel. We make the hypothesis that a boundary layer exists, the flow is laminar, two dimensional or axisymmetric and made of Ns chemically reacting perfect gas species. These assumption can look quite restrictive, ruling out fully three dimensional or turbulent flows, but are consistent with the goal of deriving an approximate analytical solution of boundary layer equations, that is subsequently used to establish the heat flux similitude criteria. Although boundary layer equations are simpler than Navier-Stokes ones, it is still impossible to determine an analytical solution valid in the general case and therefore simplifying assumptions are needed.

We apply the Lees-Dorodnitsyn coordinate transformation[2] to the boundary layer equations and write them in function of the new independent coordinates ξ (that plays the role of a transformed streamwise coordinate) and η (that plays the role of a transformed normal to the wall coordinate). The new variables are defined as: $\xi = \int_0^x \rho_\delta \mu_\delta u_\delta r^{2\epsilon} dx$, $\eta = u_\delta r^\epsilon / \sqrt{2\xi} \int_0^y \rho dy$, where $\epsilon = 1$ for axisymmetric flows and $\epsilon = 0$ for two dimensional ones. Subscript δ means boundary layer outer edge. We assume also that the mixture of Ns reacting species can be approximated with a suitable binary mixture made of atoms and diatomic molecules: such an approximation has been shown to be satisfactory for air,[3] but is clearly not satisfactory for mixtures containing carbon dioxide. The boundary layer is assumed to be

locally self-similar, i.e. all the terms, except β (to be defined later), that contain derivatives w.r.t. to the ξ variables are negligible compared to terms that contain derivatives w.r.t. to the η variable. The last approximation is still acceptable for the purpose of computing the heat flux load.[5] The simplified and transformed boundary layer equations (continuity equation is automatically taken into account in the present formulation) read:

- Species continuity

$$-f\frac{\partial y_A}{\partial \eta} - \frac{\partial}{\partial \eta}\left(l_0 \frac{Le}{Pr}\frac{\partial y_A}{\partial \eta}\right) = \frac{2\xi}{u_\delta \xi_x}\frac{\dot{w}_A}{\rho} \tag{1}$$

  ξ_x is the derivative of ξ transformed coordinate w.r.t. the original x coordinate.

- Momentum

$$-f\frac{\partial}{\partial \eta}\left(\frac{\partial f}{\partial \eta}\right) - \frac{\partial}{\partial \eta}\left[l_0 \frac{\partial}{\partial \eta}\left(\frac{\partial f}{\partial \eta}\right)\right] = \beta\left[\frac{\rho_\delta}{\rho} - \left(\frac{\partial f}{\partial \eta}\right)^2\right] \tag{2}$$

- Total enthalpy

$$-f\frac{\partial g}{\partial \eta} - \frac{\partial}{\partial \eta}\left(\frac{l_0}{Pr}\frac{\partial g}{\partial \eta}\right) = \frac{u_\delta^2}{2h_{0\delta}}\frac{\partial}{\partial \eta}\left[\frac{l_0}{Pr}(Pr-1)\frac{\partial}{\partial \eta}\left(\frac{\partial f}{\partial \eta}\right)^2\right] + \frac{\partial}{\partial \eta}\left[\frac{l_0}{Pr}(Le-1)\frac{\partial y_A}{\partial \eta}\frac{h_A - h_M}{h_{0\delta}}\right] \tag{3}$$

Subscript A designates atoms, subscript M molecules. $\dot{w}_A$ is the chemical reactions production term[2] of atoms. The term β reads:

$$\beta = \frac{2\xi}{u_\delta}\frac{du_\delta}{d\xi} = -\frac{2\xi}{\rho_\delta u_\delta^2}\frac{dp_\delta}{d\xi} \tag{4}$$

and is due to the effect of external pressure gradient. Pr is the Prandtl number, Le the Lewis number and $l_0 = \rho\mu/(\rho_\delta\mu_\delta)$ is the Chapman Rubesin number. y_A is the atom mass fraction, $\partial f/\partial\eta = u/u_\delta$ is the normalized velocity and $g = h_0/h_{0\delta}$ the scaled total enthalpy. Under the reasonable hypothesis that the Lewis number is close to one for a reacting mixture[4] and the wall is highly cooled, the last term on the r.h.s. of Eq. 3 is neglected. Lees[4] has shown that the r.h.s. can be neglected in the momentum equation (Eq. 2) if one is interested only in the heat flux evaluation. This assumption reduces the momentum equation to the well known Blasius form[8] (when $l_0 = 1$ in the boundary layer) and allows to solve analytically the species and energy equations, if l_0, Pr and Le are kept constant; resulting heat flux predictions are still satisfactory for engineering purposes.[6] The wall heat flux reads:

$$q_w = \frac{\rho_w\mu_w}{Pr}\frac{u_\delta r^\epsilon}{\sqrt{2\xi}}\left[h_{0\delta}\frac{\partial g}{\partial \eta}\Big|_w + (Le-1)\frac{\partial y_A}{\partial \eta}\Big|_w (h_{Aw} - h_{Mw})\right] \tag{5}$$

The quantity $h_{Aw} - h_{Mw}$ (difference of static enthalpy) can be approximated, when wall temperature is less than 2000 K, by Δh_{RA}, i.e. the enthalpy of formation of atomic species. The derivatives of normalized total enthalpy g and atom mass fraction y_A at the wall are obtained by solving Eqs. 1,2,3 with the following boundary conditions.

- Momentum equation.

$$f(0) = f_w = 0, \quad \frac{\partial f}{\partial \eta}(0) = \frac{\partial f}{\partial \eta}\Big|_w = 0, \quad \frac{\partial f}{\partial \eta}(\infty) = \frac{\partial f}{\partial \eta}\Big|_\delta = 1$$

- Total enthalpy equation

$$g(0) = g_w, \quad g(\infty) = g_\delta = 1$$

- Species equation

$$\frac{\partial y_A}{\partial \eta}(0) = \frac{\partial y_A}{\partial \eta}\Big|_w = \frac{k_w Pr\sqrt{2\xi}}{\mu_w Le u_\delta r^\epsilon} y_{Aw} = E_w y_{Aw} \tag{6}$$

$$y_A(\infty) = y_{A\delta}$$

k_w is the wall catalytic speed and is linked to the wall recombination probability γ by the Hertz-Knudsen relation:

$$k_w = \gamma\sqrt{\frac{kT_w}{2\pi m_A}}$$

f being known, Eqs. 1 and 3 can be solved analytically for y_A and g and their solutions read:

$$y_A(\eta) = y_{Aw} + \frac{\partial y_A}{\partial \eta}\Big|_w F_y(\eta) - \frac{Pr}{Le}\frac{2\xi}{u_\delta \xi_x} G(\eta) \tag{7}$$

$$g(\eta) = g_w + \left.\frac{\partial g}{\partial \eta}\right|_w F_g(\eta) + \frac{u_\delta^2}{2h_{0\delta}}(1 - Pr)H(\eta) \tag{8}$$

The functions $F_g(\eta)$, $F_y(\eta)$ and $H(\eta)$ involve double integrals of f and its derivatives, the function $G(\eta)$ is a double integral of the chemical reaction term $\dot{w}_A$ and f and obviously represents the effect of chemical reactions on the chemical composition. At the wall and at the boundary layer edge the above functions are equal to:

$$F_y(0) = 0,\ F_g(0) = 0,\ H(0) = 0,\ G(0) = 0$$

$$\frac{\partial F_y}{\partial \eta}(0) = 1,\ \frac{\partial F_g}{\partial \eta}(0) = 1,\ \frac{\partial H}{\partial \eta}(0) = 0,\ \frac{\partial G}{\partial \eta}(0) = 0$$

$$F_y(\infty) = \frac{1}{0.47}\left(\frac{Le}{Pr}\right)^{1/3},\ F_g(\infty) = \frac{1}{0.47Pr^{1/3}},\ H(\infty) = \frac{1}{2Pr^{1/4}},\ G(\infty) = G_\delta$$

Application of boundary conditions provides the desired wall derivatives of g and y_A.

$$\left.\frac{\partial g}{\partial \eta}\right|_w = 0.47Pr^{1/3}\left[(1 - g_w) + \frac{u_\delta^2}{4h_{0\delta}}\frac{Pr - 1}{Pr^{1/4}}\right] \tag{9}$$

$$\left.\frac{\partial y_A}{\partial \eta}\right|_w = 0.47Pr^{1/3}\frac{E_w}{Le^{1/3}E_w + 0.47Pr^{1/3}}\,(y_{A\delta} + G_\delta) \tag{10}$$

Substitution of the above expressions in Eq. 5 gives, after some algebraic rearrangement, the final heat flux form:

$$q_w = 0.332\frac{\rho_w\mu_w u_\delta r^\epsilon}{Pr^{2/3}\sqrt{\xi}}(h_{0\delta} - h_{0w})\left[1 + \frac{u_\delta^2}{4(h_{0\delta} - h_{0w})}\frac{Pr - 1}{Pr^{1/4}} + \frac{Le - 1}{Le^{1/3}}\left(1 + 0.332\left(\frac{Le}{Pr}\right)^{2/3}\frac{u_\delta r^\epsilon}{\sqrt{\xi}}\frac{\mu_w}{k_w}\right)^{-1}\frac{(y_{A\delta} + G_\delta)\Delta h_{AR}}{h_{0\delta} - h_{0w}}\right] \tag{11}$$

Eqs. 11 clearly states that heat flux is a function of total enthalpy difference between outer edge and wall, recovery factor $(Pr - 1)/Pr^{1/4}$, wall catalycity, chemical composition at the boundary layer outer edge, chemical activity G_δ inside the boundary layer and flight conditions, represented by the quantity $u_\delta r^\epsilon/\sqrt{\xi}$. One to one correspondence of these factors between flight and ground facility would ensure the desired heat flux similarity.

In the next section we will apply Eq. 11 to three different cases: stagnation point, flat plate, half sphere and we will establish heat flux similitude rules.

3. Results

3.1 Stagnation point

At the stagnation point of an axisymmetric body $u_\delta = 0$ and Eq. 11 reduces to (for a 2-D body there is a factor 0.47 instead of 0.664):

$$q_w = \frac{0.664}{Pr^{2/3}}\frac{\rho_w\mu_w}{\sqrt{\rho_\delta\mu_\delta}}\sqrt{\frac{du_\delta}{dx}}(h_{0\delta} - h_{0w})\left[1 + \frac{Le - 1}{Le^{1/3}}\left(1 + \frac{0.664}{\sqrt{\rho_\delta\mu_\delta}}\left(\frac{Le}{Pr}\right)^{2/3}\sqrt{\frac{du_\delta}{dx}}\frac{\mu_w}{k_w}\right)^{-1}\frac{(y_{A\delta} + G_\delta)\Delta h_{AR}}{h_{0\delta} - h_{0w}}\right] \tag{12}$$

The quantity du_δ/dx is the external velocity gradient at the stagnation point. Stagnation point heat flux is a function of velocity gradient, flow enthalpy, density and chemical composition at the boundary layer outer edge and of the wall enthalpy and catalycity. As a consequence, when the boundary layer conditions are the same in the wind tunnel and in flight, the heat flux is equal in the two cases (same G_δ is implied by the previous conditions). Under the somewhat restrictive assumption that the flow is near equilibrium at the boundary layer edge, it follows that the heat flux in the stagnation region is the same in flight and in the wind tunnel if total enthalpy (that, at stagnation point, coincides with static enthalpy), pressure and velocity gradient are the same at the outer edge of the boundary layer.[1]

Using the extrapolation method of Ref. 1 we establish the stagnation point heat flux similitude between a cylindrical TPS sample inside the von Karman Institute Plasmatron wind tunnel[7] and a real flying vehicle. The values of total enthalpy, pressure and velocity gradient at the stagnation point of the sample are: $h_{0\delta} = 22.8\,MJ/kg$, $p_\delta = 12525\,Pa$, $du_\delta/dx = 1502\,s^{-1}$. The corresponding flight vehicle, with the same key stagnation point parameters, has a nose radius of $1.79\,m$, flies at an altitude of $61\,km$ and a Mach number $M = 21.5$. The reacting mixture is five species air.

We show in Fig. 1 the stagnation point heat flux for the full range of wall catalycity values; the heat flux value for $\gamma = 0$ is not shown because of the logarithmic scale, but it is practically equal to the one for $\gamma = 10^{-4}$. Computed heat flux difference between Navier-Stokes and boundary layer goes from 2% for noncatalytic wall to 3% for fully

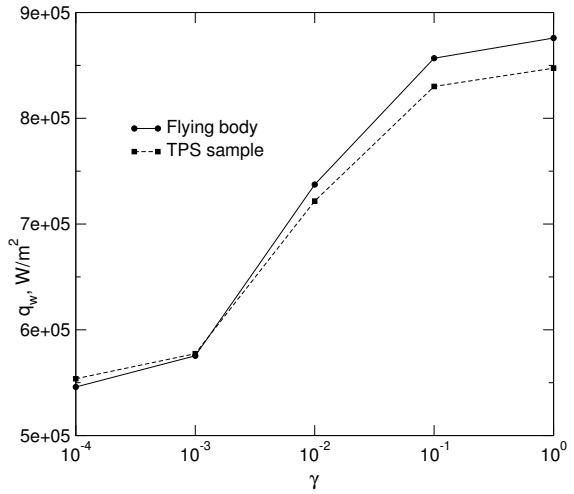

Figure 1: Stagnation heat flux for different catalycity levels

catalytic wall. The main reason of such a good agreement is that equal enthalpy, pressure and velocity gradient ensure that the same boundary layer structure is present on the sample and the flying vehicle. Stagnation point boundary layer thickness is a function of the square root of the inverse of velocity gradient[8]; in addition velocity gradient dictates the typical flow time at the stagnation point, that is the same for both configurations. Enthalpy and pressure are the same too at the boundary layer edge and therefore also the chemical characteristic time is the same. We conclude that the first Damköhler number is equal for both wind tunnel and flight and chemical composition inside the boundary layer should be close for both ground facility and flight. The above statements are validated by the profiles of oxygen and

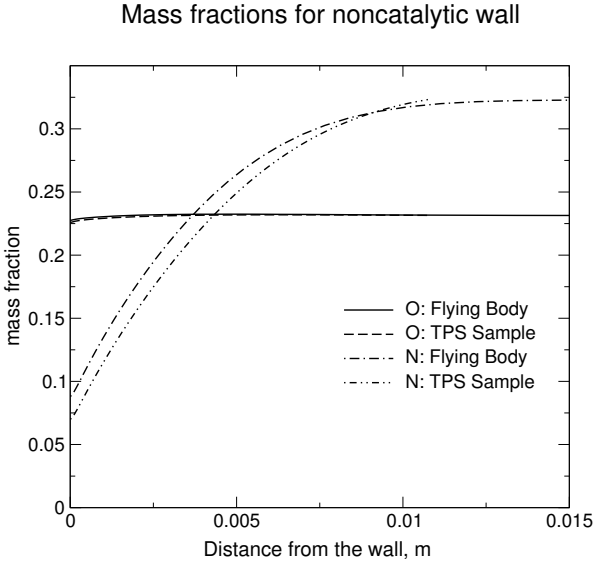

Figure 2: Stagnation point *O* and *N* mass fractions for noncatalytic wall

nitrogen shown in Fig. 2. Oxygen is fully dissociated at the boundary layer outer edge and remains fully dissociated all along the boundary layer; agreement between ground and flight profiles is excellent. Nitrogen is partially dissociated at boundary layer edge and recombines inside the boundary layer; again the agreement between ground and flight is good.

Also the second Damköhler number, which characterizes the heterogeneous chemistry-diffusion coupling and therefore the interaction between the TPS material and the reacting gas, is well reproduced. This number is defined as: $Da_2 = k_S l^2/D$ where k_s is the inverse of a characteristic time of the wall heterogeneous reactions, D a diffusion coefficient and l a characteristic length over which diffusion takes place, i.e. the boundary layer thickness. The surface material is the same and, therefore, k_s is the same too; in addition, because pressure, temperature and chemical composition are similar also D is the same. Also boundary layer thickness l is fairly close in the two configurations and we

deduce that also the second Damköhler number is acceptably duplicated in the ground facility.

3.2 Flat plate

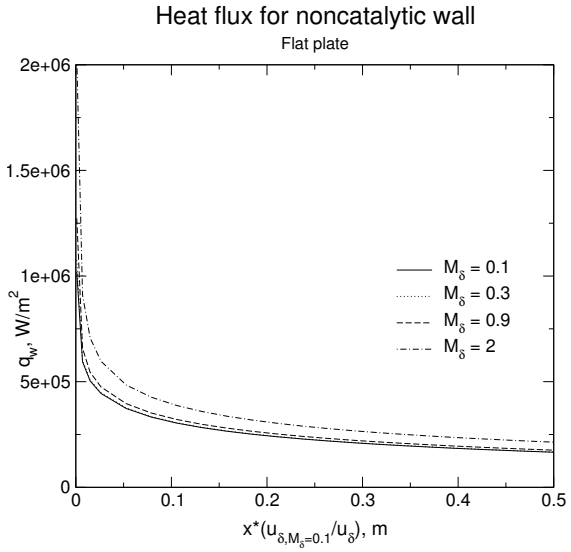

Figure 3: Flat plate heat flux: noncatalytic wall

The wall heat flux formula is similar to Eq. 11 except that the term $u_\delta r^\epsilon / \sqrt{\xi}$ is replaced by $\sqrt{u_\delta / x}$, under the hypothesis that outer edge boundary conditions are constant. Flat plate heat flux is a function of total enthalpy, velocity, density, chemical composition at the boundary layer outer edge, of the term u_δ / x (that has the dimensions of a velocity gradient) and of the wall enthalpy and catalycity. Therefore the heat flux is equal in flight and in the ground facility if the previous quantities are the same in both cases. Unfortunately equal outer edge velocity implies equal flat plate dimensions, because u_δ / x has to be the same. However, if one can tolerate a discrepancy in the heat flux, it is possible to relax the condition on velocity and to allow for different dimensions in flight and in the wind tunnel by imposing same static enthalpy, instead of total one. In order to assess our statements, the boundary layer along a flat plate is computed. The outer edge boundary conditions are as follows: $p_\delta = 12525\,Pa$, $T_\delta = 6000\,K$, $M_\delta = 0.1, 0.3, 0.9, 2$. The outer

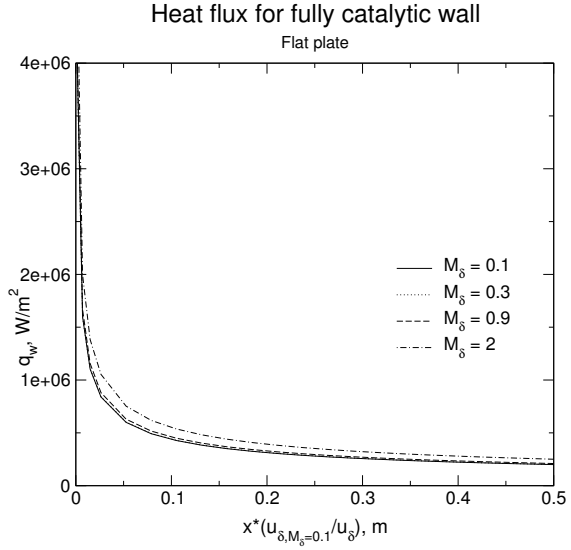

Figure 4: Flat plate heat flux: fully catalytic wall

edge chemical composition is considered to be the equilibrium one. The wall is assumed to be at radiative equilibrium and the emissivity coefficient is set to 0.85. The reacting mixture is five species air and the computations are made for

two levels of catalytic recombination probability, $\gamma = 0$ and $\gamma = 1$. In Figs. 3 and 4 the heat flux for noncatalytic and fully catalytic wall respectively is shown for all Mach numbers. The heat flux is expressed in function of the normalized coordinate $x(u_{\delta,M_\delta=0.1}/u_\delta)$ that is the same for all Mach numbers. Supposing we want to simulate the real flight flow with a Mach 0.1 wind tunnel flow, the agreement in heat flux (except for a small region near the flat plate tip, where the classical boundary layer theory is not adequate) ranges from excellent for $M_\delta = 0.1,\ 0.3,\ 0.9$ to acceptable for $M_\delta = 2$. The maximum heat flux difference for a noncatalytic wall is around 21 % between $M_\delta = 0.1$ and $M_\delta = 2$, for a fully catalytic wall it is around $18 - 19$ % for the same Mach number range. The heat flux difference is easily explained: it is due to the viscous dissipation that naturally increases with Mach number. Although the outer edge Mach number is different, the structure of the boundary layer is similar for equal values of the normalized coordinate $x(u_{\delta,M_\delta=0.1}/u_\delta)$ for all cases. Atomic oxygen and nitrogen profiles are shown in Fig. 5; only the profiles for $M_\delta = 0.1$ and $M_\delta = 2$ are shown, the ones for the remaining Mach numbers fall in between the two. The agreement is good and the boundary layer thickness is the same. In effect same u_δ/x implies same Damköhler numbers (first and second) and the same boundary layer thickness,[8] thus demonstrating the validity of our Local Heat Flux Similarity concept.

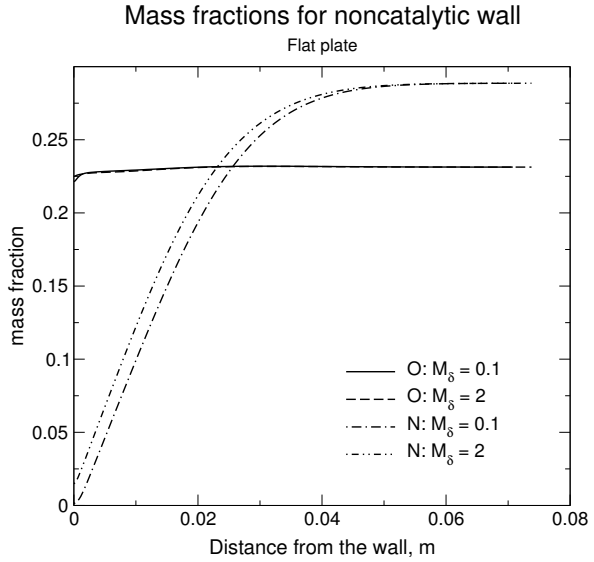

Figure 5: Flat plate O and N mass fraction at $x(u_{\delta,M_\delta=0.1}/u_\delta) = 0.5$ for noncatalytic wall

3.3 Half sphere

In this paragraph we want to explore the possibility of simulating the heat flux over the spherical front nose of a re-entry vehicle with a spherical probe inside a low Mach number wind tunnel, like for example the von Karman Institute Plasmatron[7] (inside which the Mach number is in the range $0.05-0.35$). At these regimes the plasma flow of dissociated air behaves as an incompressible flow; it is therefore reasonable to assume that, outside the boundary layer, the velocity and pressure distributions over the front half of the spherical probe itself, are given by the standard potential theory.[9]

Inspection of Eq. 11 shows that the key parameters for heat flux similitude are total enthalpy, velocity and chemical composition at the boundary layer outer edge, wall enthalpy and catalycity and the flight conditions factor $f_c = u_\delta r^\epsilon/\sqrt{\xi}$. The expression of f_c for the hypersonic flow over the spherical nose of a re-entry vehicle is given in Ref. 4. For the ground facility flow[9] $u_\delta = 3/2 u_\infty \sin(x/R)$, where u_∞ is the freestream velocity, R the spherical probe radius and x the local boundary layer streamwise coordinate. In addition $r = R\sin(x/R)$. Using a reasoning similar to the one of Ref. 4, f_c for the ground facility reads:

$$f_c^t = \frac{u_\delta r^\epsilon}{\sqrt{\xi}} \approx \frac{1}{\sqrt{\rho_{\delta s}\mu_{\delta s}}} \sqrt{\frac{du_\delta}{dx}\Big|_s} \left[2 - \left(\frac{1}{3} + \frac{3}{2}\gamma_\infty M_\infty^2\right)\frac{x^2}{R^2} + \left(\frac{1}{144} + \frac{25}{32}\gamma_\infty M_\infty^2 - \frac{27}{64}\gamma_\infty^2 M_\infty^4\right)\frac{x^4}{R^4}\right] \tag{13}$$

Subscript s means a quantity computed at the probe stagnation point, subscript ∞ refers to a freestream quantity, M is the Mach number and γ the usual specific heats ratio. The velocity gradient at the probe stagnation point is equal to[9] $3u_\infty/(2R)$.

The flight freestream conditions and body geometry are the same as in Sec. 3.1. For the wind tunnel we choose $M_\infty = 0.05$ and $M_\infty = 0.15$. The corresponding probe radiuses, computed imposing same stagnation velocity gradient in flight and in the wind tunnel, are respectively: $R = 10\,cm$ and $R = 30\,cm$.

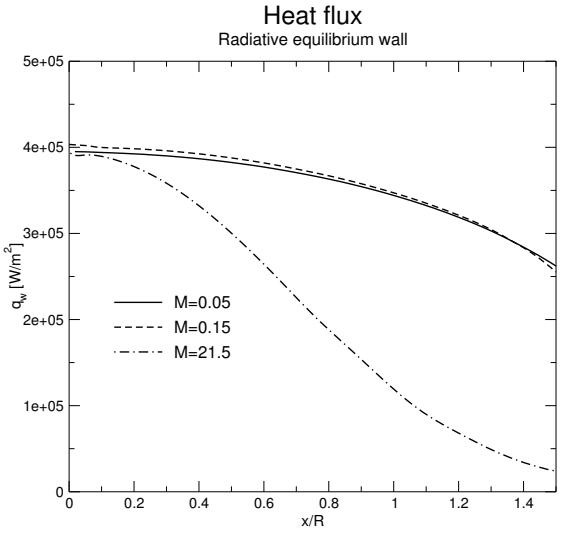

Figure 6: Half sphere heat flux: radiative equilibrium wall

In Fig. 6 the heat flux, numerically computed for a noncatalytic radiative equilibrium wall, is shown. In the stagnation point the agreement is excellent, as should be expected because we impose identical conditions. There is practically no difference in heat flux between $M_\infty = 0.05$ and $M_\infty = 0.15$: the contribution of kinetic energy to total enthalpy and therefore to heat flux is negligible. Outside the stagnation point the heat flux over the probe is higher than the heat flux over the real vehicle. For $x/R = \pi/2$ the former drops to roughly 60% of the stagnation point value, whereas the latter drops to approximately 10% of the stagnation value. However for $x/R \leq \pi/4$ results are more encouraging; probe heat flux drops to 90% of stagnation value, vehicle heat flux drops to 60% of stagnation value. The main reason of such a discrepancy is due to the f_c factor that is different for flight and wind tunnel. This is demonstrated in Fig. 7 where it is shown the normalized heat flux, that coincides practically with f_c (except for the du_δ/dx factor).

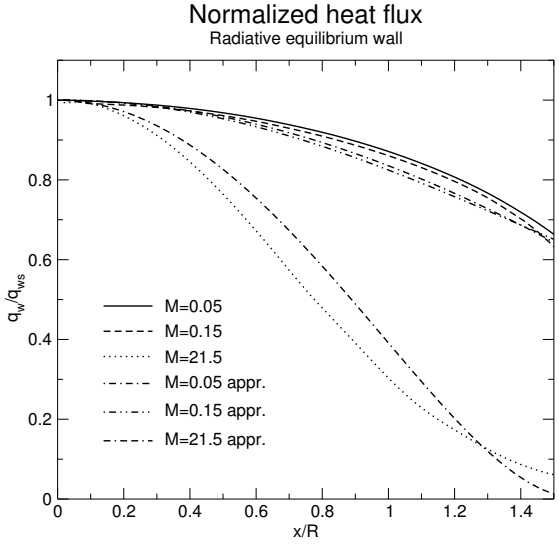

Figure 7: Half sphere normalized heat flux: radiative equilibrium wall

It is interesting to compare these "exact" numerical results with the analytical ones obtained in Ref. 4 and Eq. 13. We do this in Fig. 7 where the computed normalized heat flux (heat flux divided by stagnation point one) is shown along with the analytical one. We remark a good agreement between numerical values and analytical ones, especially for the low Mach number case. It is a remarkable demonstration of the validity of the present approach, even with all the assumptions made in order to obtain an analytical expression for the wall heat flux.

4. Conclusions

The Local Heat Flux Similarity concept, that determines the conditions for heat flux similitude between real flight and wind tunnel, has been presented with its application to three different configurations: stagnation point, flat plate and half sphere.

In the stagnation configuration, the equality of stagnation enthalpy, pressure and velocity gradient is necessary for a correct reproduction of the flight thermochemical environment inside the ground facility. Results show a good agreement between flight and ground facility for all values of wall catalycity. For the flat plate configuration, the heat flux is not duplicated as accurately as in the stagnation point configuration, however first and second Damköhler numbers are well duplicated and therefore also the chemical composition in the boundary layer and the wall heterogeneous chemical reactions phenomena. In the half sphere case, as predicted by the analytical formula, the wind tunnel heat flux is higher than the flight one; the main reason being the different velocity distribution for the two cases.

In all test cases there is a good agreement between our approximate analytical formulas, with related similarity criteria, and the “exact” numerical computations.

References

[1] Barbante P.F., Chazot O. Flight Extrapolation of Plasma Wind Tunnel Stagnation Region Flowfield. *Journal of Thermophysics and Heat Transfer*, 20:493-499, 2006.

[2] Barbante P.F., Sarma G.S.R. Computation of Nonequilibirum High-Temperature Axisymmetric Boundary-Layer Flows". *Journal of Thermophysics and Heat Transfer*, 16:490-497, 2002.

[3] Fay J.A., Riddell F.R. Theory of Stagnation Point Heat Transfer in Dissociating Air. *Journal of the Aeronautical Sciences*, 25:73-85, 1958.

[4] Lees L. Laminar Heat Transfer over Blunt-nosed Bodies at Hypersonic Flight Speeds. *Jet Propulsion*, 26:259-269, 1956.

[5] Kemp N.H., Rose R.H. and Detra R.W. Laminar Heat Transfer around Blunt Bodies in Dissociated Air. *Journal of the Aerospace Sciences*, 26:421-430, 1959.

[6] Inger G.R. Nonequilibrium Stagnation Point Boundary Layers with Arbitrary Surface Catalycity. *AIAA Journal*, 1: 1776-1784, 1963.

[7] Bottin B., Chazot O., Carbonaro M. The VKI Plasmatron Characteristics and Performance. *Measurement Techniques for High Temperature and Plasma Flows*, NATO-RTO, 1999.

[8] White F.M. Viscous Fluid Flows. *McGraw-Hill*, 1991.

[9] White F.M. Fluid Mechanics. *McGraw-Hill*, 1998.

This page has been purposedly left blank